Facial Feature Localization Using Robust Active Shape Model and POEM Descriptors

Lifang Zhou
College of Computer Science, Chongqing University, Chongqing, 400030, China
College of software, Chongqing University of Posts and Telecommunications Chongqing, 400065, China
Email: zhoulf@cqupt.edu.cn

Bin Fang
College of Computer Science, Chongqing University, Chongqing, 400030, China
Email: fb@cqu.edu.cn

Weisheng Li and Lai Peng
Institute of Computer Science and Technology, Chongqing University of Posts and Telecommunications, Chongqing 400065, China
Email: liws@cqupt.edu.cn; ivyicecream@163.com

***Abstract*—Active Shape Model (ASM) has been shown to be a powerful tool for image interpretation, especially in feature points localization for face image. The original ASM model parameter estimation is based on the assumption that the profiles follow a Gaussian distribution. Its performance is always vulnerable to distortion due to pose, illumination and expression variations. In this paper, the improvement of ASM model concerns the following two aspects. Firstly, an adaptive parameter estimation method is proposed by defining a rotation factor. Secondly, local appearances of landmarks are originally represented by Patterns of Oriented Edge Magnitudes (POEM) descriptors, which can provide more robust and accurate searching guidance than intensity profiles. The simulations are carried out using the IMM dataset, which contains 240 face images. Experimental results show that the proposed method significantly outperforms the original ASM and ASM plus LBP method under exterior variations.**

***Index Terms*—Active shape model (ASM); Patterns of Oriented Edge Magnitudes (POEM); Local binary pattern (LBP); Facial feature localization**

I. INTRODUCTION

Facial feature landmarks play a crucial role in facial information perception [1, 2]. Extensive researches have been conducted on location of facial feature, which can be divided into two categories: local methods [3, 4] and global methods [5, 6, 7]. The latter are more accurate and robust than the former because they detect facial features jointly rather than separately. Among all existing global methods, Active Shape Model (ASM) has gained much attention.

ASM is first introduced by Cootes et al. [6] and has gained great success in face research area. Two main jobs have been performed by ASM algorithm: the statistical model construction (local gray grads model and points distribution model) and feature points search (local points search and shape search). The method can be not only used for facial feature location but also utilized for face synthesis, face recognition and facial expression recognition. However, it still suffers from variations of pose, illumination, expressions and obstacles like mustaches and glasses. Furthermore, three major drawbacks, which limit its further applications to the practical face recognition are summarized as follows: 1) Initialization. Its location accuracy is sensitive to initial shape; 2) texture information. The poor texture information description of local gray grads model can result in the wrong searched candidate points; 3) searching scale. The challenge in this area is to find a good tradeoff between searching scale and searching result. Being lack of good criterion to evaluate the searching effect, it is still difficult to choose the searching scale.

To overcome the aforementioned shortcomings arising from ASM, some improvements on ASM have been made in recent years [8, 9, 10, 11]. This paper attempts to solve the above problems by presenting two improvements. Firstly, we add a rotation factor R to initialize the shape vector b in the ASM initialization process, which ensures that our extracted feature landmarks correspond well to varying poses. Secondly, local appearances of landmarks are originally represented by POEM (Patterns of Oriented Edge Magnitudes) descriptors [12, 13, 14] instead of intensity profiles. The advantages of such improvements are summarized as follows: 1) ASM model parameter estimation is based on the assumption that residuals between models have a Gaussian distribution. However, in many real applications, especially in face recognition including pose variation, this assumption may be inaccurate. Here, the adaptive parameter estimation method is shown to increase the accuracy of initialization. 2) POEM can not only characterize region information of the landmark

doi:10.4304/jcp.9.3.717-724

across different directions but also extract multi-resolution features by using different scales of cells and blocks; POEM descriptors are gradient orientation histograms based representations of image neighborhood. They are robust to exterior variations, such as pose and illumination. Hence, POEM descriptors can provide more robust and accurate guidance than intensity profiles for finding the best candidate points.

The remainder of the paper is organized as follows: Section 2 describes the details of ASM model. Section 3 introduces the rotation factor R to initialize the shape vector b in the ASM initialization process and the novel POEM feature extraction method for ASM texture information description. Section 4 presents experimental results. Section 5 concludes the paper and discusses possible future extensions.

II. Overview of ASM Algorithm

The algorithm of ASM can be divided into two steps: model construction and searching process [6]. Hence, the following section gives a brief review to the original ASM.

A. Statistical Shape Models

A shape model is described by landmark points that represent the important positions in the face to be represented. In order to generate these points, a set of training images for the given face is manually marked in the same location on the face in each image. For example, Fig. 1 shows a training image with 80 landmark points marked. The set of feature points forms a special shape, which can be represented by a shape vector:

$$s = \left(x_1, y_1, \cdots x_N, y_N \right) \tag{1}$$

We align these shape vectors by translation, scaling and rotation for minimizing the sum of squared distances between their corresponding landmark points. In most cases, two iterations of aligning algorithm are sufficient to all the shapes. Fig. 2 illustrates a small training set before and after alignment. The estimate of the mean shape $\overline{s}$ is computed using Eq. (2) and the deviation of each training shape from the mean is computed using Eq. (3). Where M denotes the number of the training shapes.

$$\overline{s} = \frac{1}{M} \sum_{i=1}^{M} s_i \tag{2}$$

$$S = \frac{1}{M} \sum_{i=1}^{M} \left(s_i - \overline{s} \right)^T \left(s_i - \overline{s} \right) \tag{3}$$

In order to capture the statistics of the shape variations, we apply Principal Component Analysis (PCA) to the data. The eigenvalues $\left(\lambda_1, \cdots, \lambda_s \right)$ and the corresponding eigenvectors $\left(p_{1,\cdots,} p_s \right)$ of the covariance matrix S, where $\lambda_i \geq \lambda_{i+1}$, can be computed. The first t eigenvectors satisfying the following equation are selected:

$$\sum_{i=1}^{t} \lambda_i \Big/ \sum_{i=1}^{s} \lambda_i \geq \alpha \tag{4}$$

Here, we set α to be 0.95. PCA allows then each shape s in the training set to be approximated using the mean shape $\overline{s}$ and a small number of parameters in a vector b:

$$s \approx \overline{s} + pb \tag{5}$$

where $p = \left(p_1, \cdots, p_t \right)$ is a set of principal components of shape variation and $b = \left(b_1, \cdots b_t \right)$ is a vector of shape parameters which can be computed as follows:

$$b = p^T \left(s - \overline{s} \right) \tag{6}$$

Eq. (5) allows us to generate new examples by varying the vector b, but the model is specific to the class of target objects that it intends to represent. Since ASM assumed a single mean shape so that it could model small deviations from mean. Moreover, when fitting the shape model to an object, the value of b is constrained to lie within the range of $[-3\sqrt{\lambda}, 3\sqrt{\lambda}]$ standard deviations. However, in many practical applications, the shape of face feature may be very different from the mean of the shape on some occasion. Or, in other words, considering that the initialization shape is mostly based on the frontal face image, the conventional ASM would fail to work when the face image is under different poses.

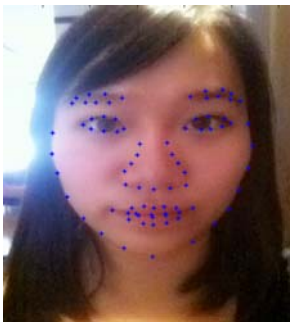

Figure 1. An example of manually location result

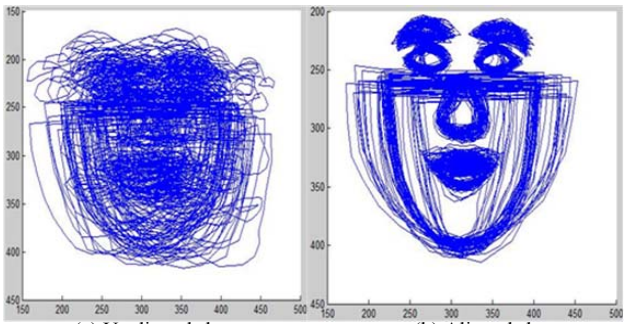

(a) Unaligned shapes (b) Aligned shapes

Figure 2. Training set before and after alignment

B. Local Appearance Models

The local appearance model, which describes the local texture feature around each landmark, is the normalized derivative of the profiles sampled perpendicular to the landmark contour and centered at the landmark [6] (Fig.

3). Furthermore, we can estimate the best position of landmarks in the searching process with the local information.

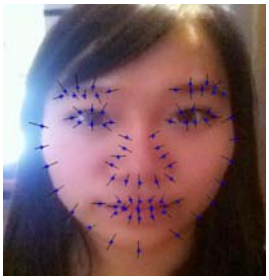

Figure 3. Profiles normal to the model boundary

The gray-level profile, g_{ij}, of the landmark j in the image i is a $(2m+1)$-D vector, in which m pixels are sampled on either side of the landmark under consideration. Eq. (7) represents the gray-level intensity of a corresponding pixel. To reduce the effect of global intensity changes, we sample the derivative along the profile, rather than the absolute gray-level values with Eq. (8). The profile is then normalized by dividing each element by the sum of absolute element values with Eq. (9).

$$g_{i,j} = \begin{bmatrix} g_{ij0} & g_{ij1} & \cdots & g_{ij(2m+1)} \end{bmatrix} \tag{7}$$

$$dg_{i,j} = \begin{bmatrix} g_{ij1} - g_{ij0} & g_{ij2} - g_{ij1} \cdots g_{ij(2m+1)} - g_{ij(2m)} \end{bmatrix} \tag{8}$$

$$y_{ij} = \frac{dg_{ij}}{\sum_{k=0}^{2m} \left| dg_{ijk} \right|} \tag{9}$$

The covariance matrix of the normalized derivative profile for M training images is

$$C_{y_j} = \frac{1}{M} \sum_{i=1}^{M} \left(y_{ij} - \overline{y}_j \right) \left(y_{ij} - \overline{y}_i \right)^T \tag{10}$$

Where $\overline{y}_j$ is the mean profile. For each landmark point j, we get a set of M normalized samples $\{y_{ij}\}$. Assuming that these samples are distributed as a multivariate Gaussian, we can compute the mean normalized derivative profile,

$$\overline{y}_j = \frac{1}{M} \sum_{i=1}^{M} y_{ij} \tag{11}$$

Given a new profile y, the quality of fitting it to its corresponding model $\overline{y}_j$ can then be computed using the Mahalanobis distance as follows:

$$f(y) = \left(y - \overline{y}_j \right)^T C_{y_j}^{-1} \left(y - \overline{y}_j \right) \tag{12}$$

During the searching process, for each landmark point, a number of sub-profiles will be generated when the best set of shape parameters is being searched. Then the sub-profiles are matched to the corresponding profiles obtained from the training set using Eq. (12). In both cases, minimizing $f(y)$ is equivalent to maximizing the probability that y comes from the distribution. In this way, a new position for each point can be obtained, and then the current pose and shape parameters are updated to match the shape model according to the suggested new points.

The local appearance models can result in a fast convergence to the local image, while the feature point will not be accurately located when the lighting conditions during searching are significantly different from the lighting conditions used to train the shape model. The reason is that the gray-level structures are very sensitive to illumination variation.

III. Our Proposed Algorithm

The above mentioned drawbacks can lead to get stuck at local minima. In this work, we propose a robust ASM model so that the problem of ASM facial feature location under pose, expression and illumination variations can be solved effectively.

A. Definition Rotation Factor of ASM

Since ASM can be viewed as a high-dimensional nonlinear optimization problem, the initialization plays an important role. In the existed initialization of ASM, the mean of the shape is usually frontal because most of the training images are frontal. However, in many cases, the input face image may be deflecting. The initial shape determined by traditional ASM may be far from the true shape in the image. A set of shape parameters $b = \left(b_1 \cdots b_t \right)^T$ is usually adopted to relieve the above problem. However, the elements of b could model only small deviations from the mean.

Fig. 4 (a) shows the mean of the shape when $b = (0,0,0,0,0,0)^T$. As can be seen from Fig. 4, the elements of b have controlled the figure variation of face image. Especially, the result after amending the first element of b can be seen in Fig. 4 (b) and (c). Obviously, it is the first element of b intimate with the pose change. Furthermore, the face image turns to the right when $b_1 > 0$, whereas it turns to the left when $b_1 < 0$.

(a) b=[0 0 0 0 0 0] (b) b=[80 0 0 0 0 0] (c) b=[-80 0 0 0 0 0]

(d) b=[0 60 0 0 0 0] (e) b=[0 -60 0 0 0 0]

Figure 4. Face shape models

In order to solve the impact of pose variation on ASM, we propose to initialize the first element of b according to the true face pose condition. Hence, we devised a rotation factor R which can judge the variation of pose change dynamically. In this paper, Adaboost algorithm [15, 16] is first used to locate two eyes, and then a projection function [17] is used to locate sideburns in order to assess facial pose. The location results of eyes and sideburns have been shown in Fig. 5. According to our observation, the ratio of the distance between eyes and sideburns vary with the attitude changes. Therefore, the rotation factor R is defined as follows:

$$R = \frac{d_1}{d_2} \tag{13}$$

Where d_1 is the distance between the centers of left eye and left sideburns and d_2 is the distance between the centers of right eye and right sideburns.

To measure the degree of pose changes, a rotation coefficient V has been further proposed. It is well known that the parameter b is limited to $[-3\sqrt{\lambda}, 3\sqrt{\lambda}]$. Since the pose changes are related to the fist element of b, so the rotation coefficient V has been defined:

$$V = \frac{\sqrt{\lambda_1}}{3} \tag{14}$$

Using the obtained rotation factor R and rotation coefficient V, the new first element of b is defined as follows:

$$b_1' = \begin{cases} VR & 1 \le R \le 9 \\ 0 & R = 1 \\ -\dfrac{V}{R} & \dfrac{1}{9} \le R < 1 \end{cases} \tag{15}$$

As a result, the proposed new initialization parameter b_1' is more adaptive to match special face shape under pose changes than the traditional parameter b_1.

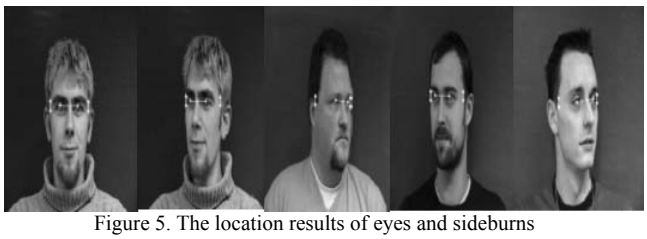

Figure 5. The location results of eyes and sideburns

B. POEM Representation of Local Appearances

The local appearance patterns are complex and it is hard to model them well only using simple profiles. Moreover, they do not contain enough information to represent widely varying local appearances of feature points under real conditions. In order to acquire abundant information related to the local gray-level structures, Keomany et al. [18] uses the points which are located within a square centered at a given landmark point to build the LBP histogram. The training step is similar to the one stated above but sampling the points in a square region rather than a profile. During searching, a LBP histogram is computed in the same way for each point located on the search profile (Fig. 6). Finally, the Chi square distance is used to compute the similarity between the testing point's histograms and the mean histogram.

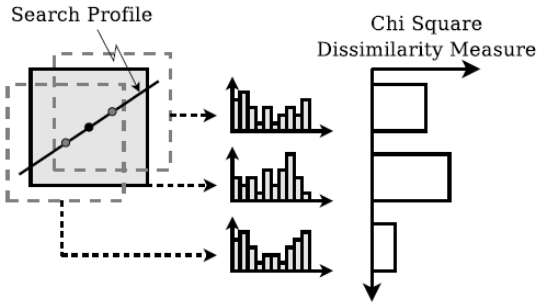

Figure 6. Search using histograms extracted from a square [18].

The square-based LBP-ASM method addresses the problem of locating facial features in frontal face images taken under different lighting conditions. However, it still suffers from variations of poses and expressions. In order to improve the robustness of original ASM algorithm to exterior variations, in this paper, local appearances of landmarks are originally represented by POEM (Patterns of Oriented Edge Magnitudes), which is a very successful local appearance descriptor developed by Vu et al. [12, 13].

Briefly speaking, for every pixel, the POEM feature is built by applying a self-similarity based structure like LBP [19, 20, 21, 22] on oriented magnitudes, calculated by accumulating a local histogram of gradient orientations over all pixels of image cells, centered on the considered pixel. The robustness and discriminative power of the POEM descriptor is evaluated than LBP, LGBP (Local Gabor Binary Patterns) and HGPP (Histogram of Gabor Phase Patterns) descriptors respectively. Furthermore, the computational cost of extracting the POEM descriptor is lower than LGBP and HGPP. Details are as follows:

Firstly, we compute the gradient image and then discretize the gradient orientation of each pixel over $(0,\pi)$ (unsigned representation) or $(0,2\pi)$ (signed representation). As shown in Fig. 7 [12, 13], for every pixel, the gradient is a 2D vector with its original magnitude and its discretized direction. In addition, at the pixel position p, a POEM feature is calculated for each discretized direction θ_i:

$$POEM_{L,w,n}^{\theta_i}(p) = \sum_{j=1}^{n} f\left(S\left(I_p^{\theta_i}, I_{c_j}^{\theta_i}\right)\right)2^j \tag{16}$$

Where I_p and I_{c_j} are the accumulated gradient magnitudes of central pixel p and surrounding pixels c_j; L and w are the sizes of blocks and cells, respectively; the number of pixels surrounding the considered pixel p is represented by n which is set to 8

here; $S(.,.)$ is the similarity function which represents the difference of two gradient magnitudes; f is defined as :

$$f(x)=\begin{cases}1 & if \quad x \geq \mathrm{T} \\ 0 & if \quad x<\mathrm{T}\end{cases} \tag{17}$$

Where T is slightly larger than zero so that the stability in uniform regions can be guaranteed. Lastly, the unidirectional POEMs at each of m orientations is been concatenated so that the final POEM feature set at each pixel can be attained.

$$POEM_{L,w,n}(p)=\left\{POEM^{\theta_1},\cdots POEM^{\theta_m}\right\} \tag{18}$$

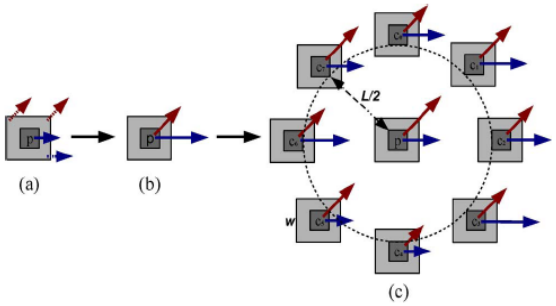

Figure 7. Main steps of POEM feature extraction [12, 13].

In our work, we originally apply POEM descriptors to represent local appearances of facial landmarks. However, being lack of spatial information, the resulting histogram will always look similar. Here, in order to retain spatial information, we divide the square into 4 regions from which the POEM histograms are extracted and concatenated into a single feature histogram representing the local appearance patterns. Finally, the average histogram of every landmark from M training samples act as the texture model. During the search step, a POEM histogram is computed in the same manner for each point. The similarity between the histograms of testing points and the mean histogram is also measured using the Chi square distance. The smaller the distance is, the more similar the histograms are.

IV. Experimental Results and Discussion

In order to evaluate the accuracy of our proposed algorithm, the average error function, Err , is defined as follows:

$$Err=\frac{1}{N}\sum_{j=1}^{N}\sqrt{\left(x_r-x_r'\right)^2+\left(y_r-y_r'\right)^2} \tag{19}$$

Err represents the distance between the landmark points searched by the algorithms and their actual positions. Where N is the total number of points used in face model, (x_r, y_r) represents the correct position of the landmark points for a face image, $(x_r, y_r)'$ is the corresponding positions obtained by the algorithmic landmark.

The comparison experiments are performed with the IMM face database, which contains 240 face images of 40 men and women. The facial images of each subject are taken with varying head pose, facial expressions and illumination. We divide the dataset into two parts: one is the training set containing 180 face images; the others act as the testing set. Some original sample images of IMM dataset are shown in Fig. 8. There are also some parameters need to be set. The 25×25 patch is chosen to extract the POEM features, and the size of block and cell is set to 6 and 3, respectively. The number of orientations is 3.

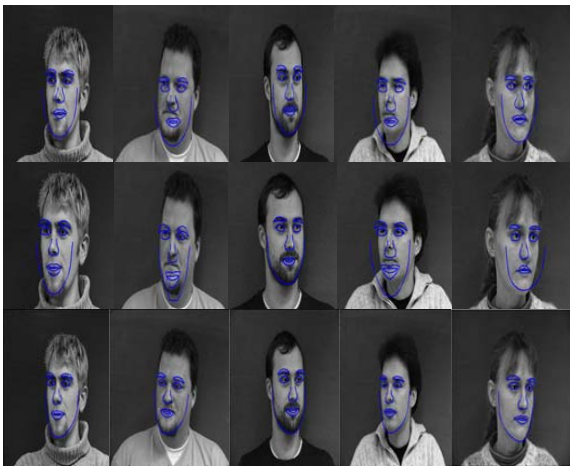

Figure 8. Some samples of IMM dataset.

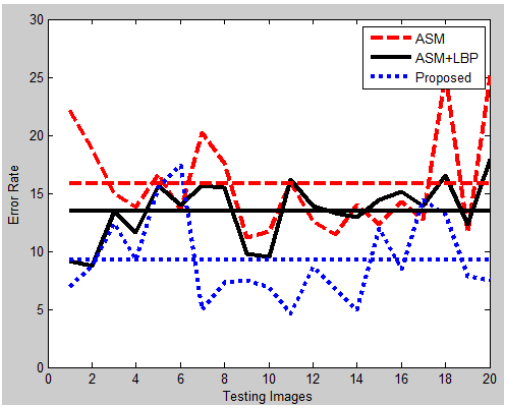

Figure 9. Error rate under pose variation

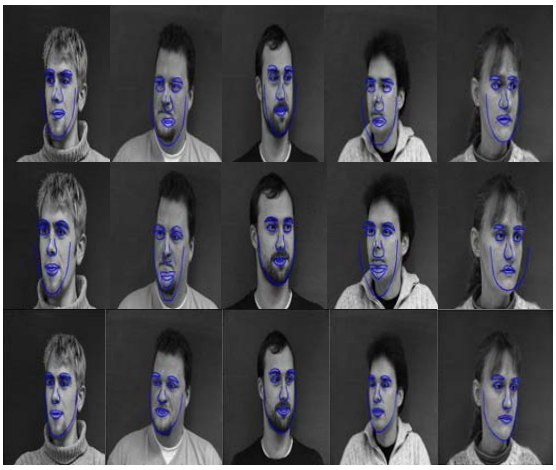

Figure 10. The searching results under pose variation by ASM (first row) , ASM+LBP (second row) and the proposed method (third row)

Four experiments are conducted. The first experiment compares the performance of the original ASM, ASM+LBP and our algorithm with the face images including pose variation. Some resulting images are shown in Fig. 9 and Fig. 10. We can find that the mean error rate of our method and ASM+LBP are 9.8% and 14%, respectively, which is less than 16% obtained by original ASM. It can be seen that the influence of texture information including LBP and POEM is evident for the accuracy of location. Furthermore, the rotation factor R plays an important role to offset pose variation. Fig. 10 shows the resulting images by ASM, ASM+LBP and the proposed method under pose variation.

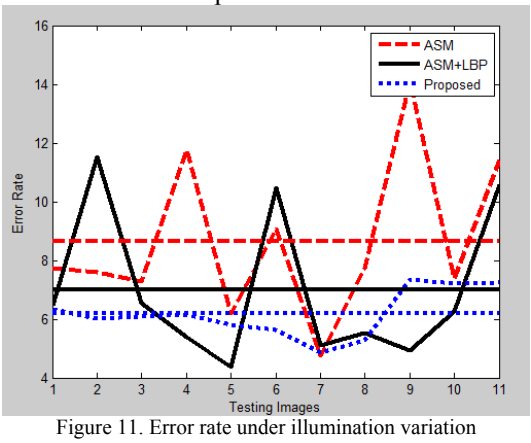

Figure 11. Error rate under illumination variation


Figure 12. The searching results under illumination variation by ASM (first row) , ASM+LBP (second row) and the proposed method (third row)

The second comparison analysis is the performance under illumination variation. The analytical data is shown in Fig. 11. As stated above, POEM descriptor is an oriented, spatial multi-resolution descriptor capturing rich information about the original image, and also is a multi-scale self-similarity based structure that results in robustness to exterior variations. This leads to the decrease of the mean error rate of the original ASM and ASM+LBP by 2.6% and 1.2%, respectively. Furthermore, we can conclude the POEM's resistance to illumination variation is stronger than LBP. Lastly, we can find from the resulting images shown in Fig. 12, the result of the proposed method is more accurate than the original ASM and ASM+LBP methods under illumination variation.

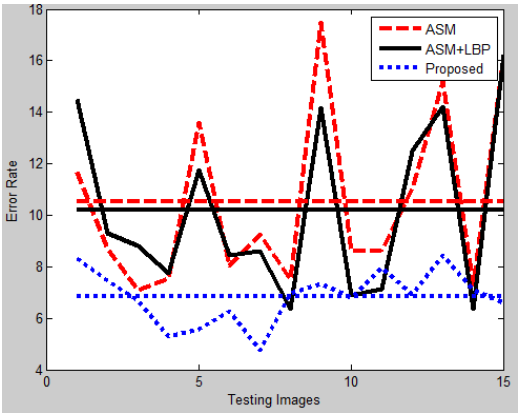

Figure 13. Error rate under expression variation

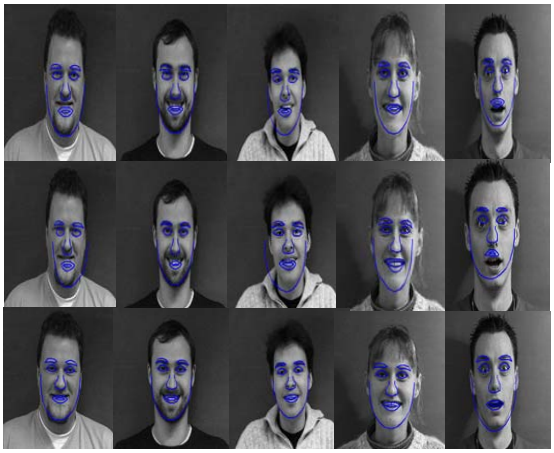
Figure 14. The searching results under expression variation by ASM (first row) , ASM+LBP (second row) and the proposed method (third row)

In the third experiment, we also select set of IMM dataset to test our method on expression variation. The results are illustrated in Fig. 13. We can find that the proposed method can enhance the accuracy of the original ASM by 3.4%. However, the average point displacement error of ASM+LBP is only 0.2% lower than that of the ASM method. More information is embedded in the construction of the local structure by POEM, which enhances the robustness and discriminative power of descriptor than LBP. Fig. 14 shows the resulting images of original ASM, ASM+LBP and the proposed method respectively.

Some other complicated conditions are selected for performance comparison. The testing face images are with different pose, different illumination and different expression. By using 50 testing images in the experiments, the overall average errors of ASM, ASM+LBP and our proposed approach are shown in Fig. 15. Some results based on these three methods are illustrated and compared in Fig. 16. These results show that the locations achieved by our approach are more accurate than those achieved by ASM and ASM+LBP. Our algorithm not only employs factor R but also uses POEM descriptor to represent the local appearances of landmarks. This can therefore provide an adaptive shape model and a more effective search for the optimal solution.

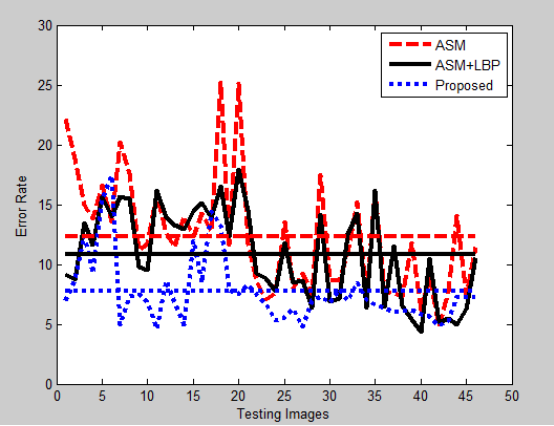

Figure 15. Error rate under complicated condition

Figure 16. The searching results under complicated condition by ASM (first row) , ASM+LBP (second row) and the proposed method (third row)

V. CONCLUSIONS

We present a robust ASM model for facial feature localization. Our method is robust to the variations of pose, illumination and expression. The main contributions of this paper include: 1) introducing a novel rotation factor R that can be used to initialize the vector of shape parameters b. 2) originally adopting the POEM descriptor to represent the local appearances of landmarks. The experimental results demonstrate that the proposed model is robust to the variation of pose, illumination and expression. Future work may focus on explaining the result of ASM for face recognition.

ACKNOWLEDGMENT

This work is supported by the Program for Natural Science Foundation of China (Nos. 61100114, 61173129, 61272195, 61171060, 61201383), the Specialized Research Fund for the Doctoral Program of Higher Education of China (No. 20120191110026), the Natural Science Foundation Project of CQ CSTC (CSTC2012JJA1699), the Program for New Century Excellent Talents in University under Grant NCET-11-1085 and the Fundamental Research Funds for the Central Universities (No. CDJXS11182240, CDJXS10182216).

REFERENCES

[1] T. Lee, S.K. Park and M. ParkAn, "Effective method for detecting facial features and face in human-robot interaction", *Inf. Sci.*, vol. 176, no. 21, pp. 3166-3189, 2006.

[2] S.H. Leung, S.L. Wang, and W.H. Lau, "Lip image segmentation using fuzzy clustering incorporating an elliptic shape function", *IEEE Trans. Pattern Anal. Mach. Intell.*, vol. 13, no. 1, pp. 51-62, 2004.

[3] G.C. Feng and P.C. Yuen, "Multi-cues eye detection on gray intensity images", *Pattern Recognit.*, vol. 34, no. 5, pp. 1033-1046, 2001.

[4] F.Y. Shih and C.F. Chuang, "Automatic extraction of head and face boundaries and facial features", *Inf. Sci.*, vol. 158, pp. 117-130, 2004.

[5] T.F. Cootes, G.J. Edwards, and C.J. Taylor, "Active Appearance Models", *IEEE Trans. Pattern Anal. Mach. Intell.*, vol. 23, no.6, pp. 681-685, 2001.

[6] T.F. Cootes, C.J. Taylor, D.H. Cooper and J.Graham, "Active Shape Models-Their Training and Application" *Comput. Vis. Image Underst.*, vol. 61, no.1, pp. 38-59, 1995.

[7] S.C. Yan, C. Liu, S.Z. Li, H.J. Zhang, H.Y. Shum, and Q.S. Cheng, "Face Alignment Using Texture-Constrained Active Shape Models", *Image Vis. Comput.*, vol. 21, no.1, pp. 69-75, 2003.

[8] G. Hamarneh, T. Gustavsson, "Deformable spatio temporal shape models: extending active shape models to 2D + time", *Image Vis. Comput.*, vol. 22, no. 6, pp. 461-470, 2004.

[9] J. Kim, M. Cetin, A.S. Willsky, "Nonparametric shape priors for active contour-based image segmentation", *Signal Process.*, vol.87, no. 12, pp. 3021 – 3044, 2007.

[10] K.W. Wan, K.M. Lam, K.C. Ng, "An accurate active shape model for facial feature extraction", *Pattern Recognit. Lett.*, vol.26, no. 15, pp. 2409 – 2423, 2005.

[11] W. Wang, S. Shan, W. Gao, B. Cao, "An improved active shape model for face alignment", in *The Fourth International Conference on Multi-modal Interface*, Pittsburgh, USA, 2002, pp. 523-528.

[12] N.S. Vu and A. Caplier, "Enhanced patterns of oriented edge magnitudes for face recognition and Image matching", *IEEE Trans. Image Process.*, vol. 21, no. 3, pp. 1352-1365, 2012.

[13] N.S. Vu and A. Caplier, "Face Recognition with Patterns of Oriented Edge Magnitudes", in *Proceeding of ECCV Conference*, pp. 313-326, 2010.

[14] N. Dalal and B. Triggs, "Histograms of oriented gradients for human detection", in *Proceeding of CVPR Conference*, pp. 886-893, 2005.

[15] Y.W. Wu and X.Y. Ai, "Face detection in color images using AdaBoost algorithm based on skin color information", in *Proceedings of the First International Workshop on Knowledge Discovery and Data Mining*, pp. 339-342, 2008.

[16] Y. Wei, X. Bing and C. Chareonsak, "FPGA implementation of AdaBoost algorithm for detection of face biometrics", in *Proceedings of IEEE International Workshop on Biomedical Circuits and Systems*, pp. 1-6, 2004.

[17] G.C. Feng and P.C. Yuen, "Variance projection function and its application to eye detection for human face recognition", *Pattern Recognit. Lett.*, vol. 19, no. 9, pp. 899-906, 1998.

[18] J. Keomany, S. Marcel, "Active shape models using Local Binary Patterns", RR 06-07, IDIAP Research institute, 2006.
[19] T. Ahonen, A. Hadid and M. Pietikainen, "Face recognition with local binary patterns", in *Proceeding of ECCV Conference*, pp. 468-481, 2004.
[20] T. Ahonen, A. Hadid and M. Pietikainen, "Face description with local binary patterns: Application to face recognition", *IEEE Trans. Pattern Anal. Mach. Intell.*, vol. 28, no.12, pp. 2037-2041, 2006.
[21] X. Li, J. Li, "LPT Optimization Algorithm in the Nuclear Environment Image Monitoring", *Journal of Software*, vol. 8, no.3, pp. 659-665, 2013.
[22] Y. Lan, Y. Zhang and H. Ren, "A Combinatorial K-View Based algorithm for Texture Classification", *Journal of Software*, vol. 8, no.1, pp. 218-227, 2013.

Lifang Zhou received her M.S. degree from the Chongqing University of posts and Telecommunications, Chongqing, China. She is a Lectorate of Chongqing University of Posts and Telecommunications. She is currently working towards her Ph.D. at the College of Computer Science, Chongqing University. Her research focuses on pattern recognition and machine vision, etc.

Bin Fang received his B.S. degree in Electrical Engineering from Xi'an Jiaotong University, Xi'an, China, his M.S. degree in Electrical Engineering from Sichuan University, Chengdu, China, and his Ph.D. in Electrical Engineering from the University of Hong Kong, Hong Kong, China. He is currently a Professor in the School of Computer Science, Chongqing University, China. His research interests include computer vision, pattern recognition, medical image processing, biometrics applications, and document analysis. He has published more than 100 technical papers and is an Associate Editor of the International Journal of Pattern Recognition and Articial Intelligence. He is also a senior member of IEEE.

Weisheng Li graduated from the School of Electronics and Mechanical Engineering at Xidian University in July 1997. He received his M.S. degree and Ph.D. from the School of Electronics and Mechanical Engineering and School of Computer Science and Technology at Xidian University in July 2000 and July 2004, respectively. Currently he is a Professor at Chongqing University of Posts and Telecommunications. His research focuses on intelligent information processing and pattern recognition.

Lai Peng received her B.S. degree in Information Security from Chongqing University of Posts and Telecommunications, Chongqing, China. She is currently a graduate student at the Institute of Computer Science and Technology, Chongqing University of Posts and Telecommunications, China. Her research interests include pattern recognition and machine vision.